

Pulsed Infrared Laser Inducement of Multiple Reaction Channels in Ethyl 3-Cyclohexene-1-carboxylate

D. W. Setser, Hanh H. Nguyen, and Wayne C. Danen*

Department of Chemistry, Kansas State University, Manhattan, Kansas 66506 (Received: August 11, 1982)

The pulsed CO₂ laser-induced reaction of ethyl 3-cyclohexenecarboxylate, a large organic ester with two reaction channels differing by ~13 kcal mol⁻¹ in threshold energies, was studied over the 0.02–0.20-torr pressure range. The absorbed laser energy and the reaction probabilities were measured as functions of laser energy, laser intensity, and added bath gas. The reaction product ratio was very dependent on the incident laser energy but almost independent of the laser pulse duration (intensity) at constant fluence. The dependence of the product ratio on the absorbed energy was satisfactorily explained for low fractional reaction by a postpulse model using RRKM rate constants and a broad distribution function (simulated as a Boltzmann distribution) with mean energy equal to the absorbed laser energy. In addition to implying that the internal energy is randomly distributed prior to reaction, the model implies that all, or nearly all, of the molecules absorb the laser energy. Addition of bath gas significantly lowered the reaction probability but had only a minor influence on the product partitioning ratio; these results were also interpreted satisfactorily by the model calculations. The laser-driven secondary reaction of the ethyl acrylate product, even for single-pulse experiments, is important.

Introduction

Pulsed infrared laser photochemistry has been widely investigated in recent years and the field has been reviewed.¹⁻¹¹ Interest has been directed toward the basic nature of the multiphoton absorption process, the molecular energy distributions from laser absorption, the laser-driven elementary reactions, and applications to isotope separation and sample purification. A principal reason for the interest in pulsed infrared laser-induced chemistry is the contrast to conventional thermal activation even though with both methods the main reaction usually occurs via the lowest-energy pathway. With the pulsed infrared laser-induced technique, the energy initially is deposited exclusively as vibrational energy, providing there are no collisions during the laser pulse. Most multiphoton infrared laser excitation studies have been interpreted in terms of randomization of the laser energy prior to reaction, although there are a few claims for restricted rates of energy redistribution.¹²⁻¹⁵ Even with energy random-

ization, a certain reaction selectivity is possible for competing exit channels in the same molecule; e.g., a channel with a high E_a and high A factor can be made competitive with a channel of lower E_a and A factor.^{2,16-18} Also, it is possible to generate a thermally reactive product from a comparatively stable precursor¹⁸ and to exert control over the nonequilibrium distribution of isomeric compounds.¹⁹⁻²¹

We have been concerned with the infrared laser-induced multiphoton chemistry of relatively large compounds.^{1,22,23} Some of the characteristic features of large molecules can be summarized as follows:

(1) The high density of vibrational states for 300 K samples allows the molecules to be in or nearly in the quasi-continuum after the absorption of a single infrared photon.

(2) Large molecules frequently exhibit high reaction probabilities even though their absorption cross sections are low.

(3) The rate constants of large molecules excited to a few kcal mol⁻¹ above their threshold energy are quite small and large amounts of energy must be absorbed to induce reaction.

(4) Collisional quenching by *unexcited* reactant molecules or bath gas molecules can compete efficiently with reaction, particularly at low or moderate laser fluences.

(5) For reaction probabilities of ≤10% per pulse, the majority of the reaction occurs after the laser pulse. The postpulse reaction is governed by competition between unimolecular reaction and quenching via a complex interplay of cooling processes.

(1) Danen, W. C.; Jang, J. C. "Laser-Induced Chemical Processes"; Steinfeld, J. I., Ed.; Plenum Press: New York, 1981; Vol. 1, Chapter 2.

(2) Danen, W. C. *Opt. Eng.* 1980, 19, 21.

(3) Ambartzumian, R. V.; Letokhov, V. S. In "Chemical and Biochemical Applications of Lasers"; Moore, C. B., Ed.; Academic Press: New York, 1977; Vol. III, pp 167-316.

(4) Letokhov, V. S.; Moore, C. B. In ref. 3, pp 1-165.

(5) Fuss, W.; Kompa, K. I.; Proch, D.; Schmid, W. E. "Lasers in Chemistry"; West, M. A., Ed.; Elsevier: Amsterdam, 1977; 235-44.

(6) Grunwald, E.; Dever, D. F.; Keehn, P. M. "Megawatt Infrared Laser Chemistry"; Wiley: New York, 1978.

(7) N. Bloembergen, N.; Yablonovitch, E. *Phys. Today* 1978, 31, 23.

(8) Cantrell, C. D.; Freund, S. M.; Lyman, J. L. "Laser Handbook"; Sticht, M. L.; Noth-Holland Publishing Co.: Amsterdam, 1979; Vol. III.

(9) Kompa, K. I.; Fuss, W.; Proch, D.; Schmid, W. E.; Smith, D. S.; Schroder, H. "Nonlinear Behavior of Molecules, Atoms, and Ions in Electric, Magnetic, or Electromagnetic Fields"; Elsevier: Amsterdam, 1979; pp 55-63.

(10) Ronn, A. M. *Sci. Am.* 1979, 240, 114.

(11) Schulz, P. A.; Sudbo, A. S.; Krajnovich, D. J.; Kwok, H., S.; Shen, Y. R.; Lee, Y. T. *Annu. Rev. Phys. Chem.* 1980.

(12) (a) Brenner, D. M. *Chem. Phys. Lett.* 1978, 57, 357. (b) Brenner, D. M. *J. Phys. Chem.* 1982, 41. The more recent discussion of the power-dependent product branching ratio for ethyl vinyl ether is based on laser pumping rates rather than slow intramolecular energy relaxation.

(13) Kaldor, A.; Hall, R. B.; Cox, D. M.; Horsley, J. A.; Rabinowitz, P.; Kramer, G. M. *J. Am. Chem. Soc.* 1979, 101, 4465.

(14) Cox, D. M.; Hall, R. B.; Horsley, J. A.; Kramer, G. M.; Rabinowitz, P.; Kaldor, A. *Science* 1979, 205, 390.

(15) Hall, R. B.; Kaldor, A. *J. Chem. Phys.* 1979, 70, 4027.

(16) Reiser, C.; Lussier, F. M.; Jensen, C. C.; Steinfeld, J. I. *J. Am. Chem. Soc.* 1979, 101, 350.

(17) Lussier, F. M.; Steinfeld, J. I. *Chem. Phys. Lett.* 1977, 50, 175.

(18) Danen, W. C.; Nguyen, H. H. *J. Am. Chem. Soc.*, in press.

(19) Glatt, I.; Yogeve, A. *J. Am. Chem. Soc.* 1976, 98, 7087.

(20) Yogeve, A.; Benmair, R. M. *J. Chem. Phys. Lett.* 1977, 46, 290.

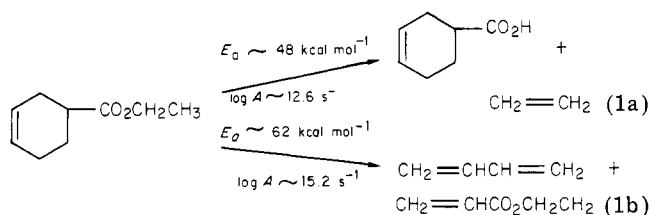
(21) Buechele, J. L.; Weitz, E.; Lewis, F. D. *J. Am. Chem. Soc.* 1979, 101, 3700.

(22) Rio, V. C.; Setser, D. W.; Danen, W. C. *J. Am. Chem. Soc.* 1982, 104, 5431.

(23) Jang, J. C.; Setser, D. W.; Danen, W. C. *J. Am. Chem. Soc.* 1982, 104, 5440.

(6) The vibrational heat capacity of the molecules is so large that $V \rightarrow T, R$ collisional energy equilibration results in only a relatively small decrease of the effective vibrational temperature.

We wish to report the pulsed infrared laser-induced reaction of ethyl 3-cyclohexene-1-carboxylate, which has two unimolecular channels with different threshold energies and A factors (eq 1a and 1b). The two channels offer



the opportunity to study the multiphoton absorption/reaction process from the perspective of both the absolute reaction probability and the channel partitioning ratio. The product ratios and absolute reaction probabilities were measured at 0.05 torr; the absolute energy and cross sections were obtained over the pressure range of 0.02–0.25 torr. The product ratio was very dependent on the incident laser energy but not affected by variation in the laser pulse duration (intensity) at constant fluence. The dependence of the product ratio on absorbed energy was satisfactorily explained by a postpulse model using RRKM rate constants and a broad distribution defined by assigning the measured absorbed energy as the mean energy of a Boltzmann distribution. The laser-driven secondary reaction of ethyl acrylate, even for single-pulse experiments, was observed. The variation of the reaction probability and the product branching ratio was studied with added He, CF_4 , and $i\text{-C}_3\text{H}_7\text{Br}$.

Experimental Section

Experiments were performed with a Lumonics Model 103 TEA pulsed CO_2 laser; the 1045.02-cm^{-1} line (P(22) of the $9\text{-}\mu\text{m}$ band) mainly was used. The laser energy was measured with a Scientech Model 380102 volume-absorbing disk calorimeter and Model 36-2002 power and energy indicator. An aperture of appropriate diameter placed outside the laser cavity was used to select the beam size and beam areas were determined by means of heat-sensitive paper. The beam profile was virtually flat (better than 90%) as measured by moving a pinhole aperture across the diameter of the beam. The maximum output of the unfocused laser beam was $\sim 2 \text{ J cm}^{-2}$. Fluences less than 2 J cm^{-2} were obtained by attenuation with Saran plastic film, and fluences greater than 2 J cm^{-2} were obtained by focusing with a 50-cm focal length BaF_2 lens or by a Galilean telescope consisting of a 75-cm focal length converging BaF_2 lens placed 37.5 cm in front of a 37.5-cm focal length diverging BaF_2 lens (Unique Optical). All experiments were done with constant geometric fluence throughout the cell. Except for energy absorption measurements, the energy removed from the laser beam by the 0.05-torr samples is negligible and the incident fluence, ϕ , is also the fluence for the whole sample.

Cells were made of Pyrex tubing fitted with polished NaCl windows. Cell lengths varied from 1 to 36 cm; cell diameters were approximately 2 times the beam diameter to minimize possible wall effects.

Analysis of the C_2H_4 , C_4H_6 , and ethyl acrylate products was accomplished with gas chromatography using a flame ionization detector; the peak areas were corrected for detector response. A $5 \text{ ft} \times 1/8 \text{ in.}$ Porapak Q column was used for analysis. The response of the detection system

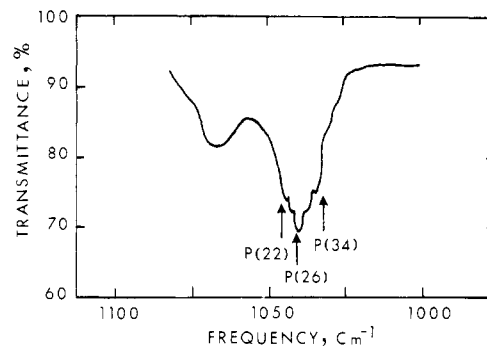


Figure 1. Infrared spectrum of ethyl 3-cyclohexene-1-carboxylate for 0.23 torr and 1-m path length. Arrows mark frequencies of laser irradiation.

was calibrated with real samples for the three products. The starting compound and the 3-cyclohexene-1-carboxylic acid were not measured since these compounds were not eluted from the column at reasonable temperatures.

The parent ester as synthesized from 3-cyclohexene-1-carboxylic acid (Fluka) by conversion to the acyl halide with thionyl chloride followed by reaction of the acyl halide with absolute ethanol in the presence of pyridine. The boiling point was 194–195 °C; GLPC analysis showed >99% purity. The vapor pressure at room temperature is 0.30 torr. The infrared spectrum ($1000\text{--}1100 \text{ cm}^{-1}$) taken by a Digilab Fourier transform infrared spectrometer with 0.23 torr in a 1-m cell is shown in Figure 1.

Energy absorption measurements were performed as described elsewhere.²² The absorption was sufficiently strong that measurements at 0.02–0.25 torr could be made with long path length cells.

Results

Product Ratio and Reaction Probability. The reaction probability, $P(\phi)$, is plotted vs. laser fluence, ϕ , in Figure 2; data were taken for three frequencies for short and long pulses and at three pressures of parent. The reaction probability is defined as the fractional reaction, based on ethylene from reaction 1a plus butadiene from reaction 1b, in the irradiated volume. The reaction probability has little dependence on wavelength, pulse length at constant ϕ , or upon pressure of the parent. The reaction probability is a strong function of ϕ and approaches unity at $\phi = 4\text{--}5 \text{ J cm}^{-2}$. The general form of the plot shown in Figure 2 is typical of the CO_2 infrared laser-induced reactions of organic esters.^{22,23} The low vapor pressure of the carboxylate restricts the pressure range of neat samples that can be investigated. Nevertheless, $P(\phi)$ was constant over the 0.02–0.2-torr pressure range at constant ϕ . This should be contrasted to the strong quenching observed when isopropyl bromide was added in the same pressure range, vide infra.

A test for thermally augmented unimolecular reaction was made with the thermal monitor technique.^{1,22,24} Isopropyl bromide ($E_a = 47.8 \text{ kcal mol}^{-1}$, $\log A = 13.6 \text{ s}^{-1}$) was chosen because of similarities in Arrhenius parameters to reaction 1a. A thermally equilibrated 1:1 mixture of isopropyl bromide and the carboxylate would produce $k_{i\text{-PrBr}}/k_1 \sim 5$ and 7 at 500 and 1000 K, respectively. The effects of adding isopropyl bromide with total constant pressure are summarized in Table I for various concentrations of isopropyl bromide. The [propylene]/[ethylene + butadiene] ratio is very low and below 0.1 torr the thermally driven component is negligible (<5%). These

(24) Danen, W. C.; Munslow, W. D.; Setser, D. W. *J. Am. Chem. Soc.* 1977, 99, 6961.

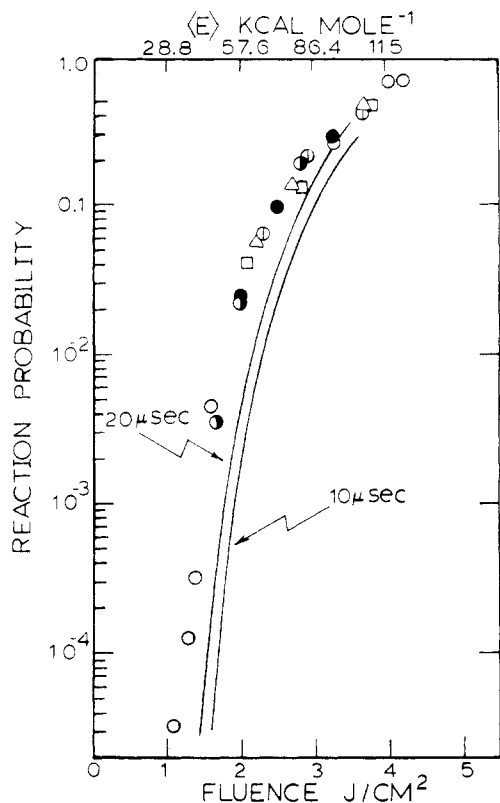


Figure 2. Reaction probability (fractional yield of ethylene and 1,3-butadiene per pulse in the irradiated volume) vs. fluence at different frequencies and pressure: (○) 1045.02 cm^{-1} , long pulse 0.02 torr; (○) 1045.02 cm^{-1} , long pulse, 0.005 torr; (●) 1045.02 cm^{-1} , short pulse, 0.05 torr; (⊙) 1045.02 cm^{-1} , long pulse, 0.10 torr; (Δ) 1041.28 cm^{-1} , long pulse, 0.25 torr; (□) 1033.49 cm^{-1} , long pulse, 0.05 torr. The absorber laser energy, $\langle E \rangle = \sigma_L \phi$, is shown in the top scale. The ethylene yield has been corrected for secondary reaction; see text. The curves are calculated yields vs. $\langle E \rangle$ for the specified lengths of time for the cooling wave from eq 7 of the text; the $A_{1b}^0 = 7 \times 10^{14}$ model was used for channel 1b.

TABLE I: Effect of Added Thermal Monitor (Isopropyl Bromide) on $P(\phi)$

ϕ , J cm^{-2}	$\text{CH}_3\text{CHBrCH}_3$, %	$P(\phi)$ - [C_3H_6]	$P(\phi)$ - [$\text{C}_2\text{H}_4 +$ C_4H_6]	$P(\phi)$ - [C_3H_6 + C_4H_6] ^a
(A) Total Pressure = 0.10 torr				
4.3	0	0.0	0.87	0.0
4.4	32	0.036	0.87	0.042
4.3	63	0.0083	0.70	0.012
3.5	37	0.015	0.42	0.035
2.7	39	0.0025	0.089	0.003
2.7	46	0.008	0.069	0.012
2.1	41	0.0052	0.011	0.047
1.7	32	0.00009	0.0011	0.079
(B) Total Pressure = 0.050 torr				
3.7	50	0.0023	0.55	0.004
2.7	26	negligible		

^a A thermally equilibrated system comprising 50% isopropyl bromide would give a ratio of 5-7.

results are similar to other studies with large organic esters²² and corroborate the necessity of utilizing pressures ≤ 0.1 torr to avoid significant thermal augmentation of reaction yield.

Experiments initially were done with the unfocused laser beam at the three frequencies noted in Figure 1 to determine the most efficient laser line. Similar conversions per laser pulse were observed at 1033.5 cm^{-1} (P(34)), the low-frequency region of the absorption band, 1041.3 cm^{-1} (P(26)), near the absorption maximum, and 1045.0 cm^{-1}

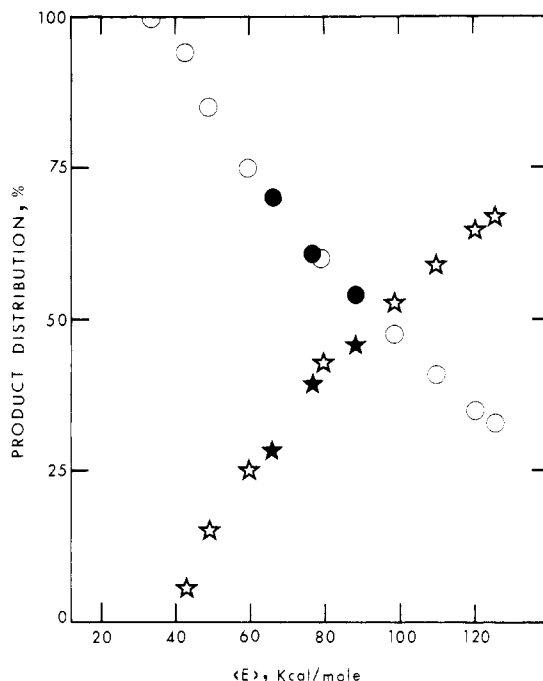


Figure 3. Product branching fractions of channels 1a and 1b vs. average energy for 1045.02- cm^{-1} irradiation at 0.05 torr: (● and ○) ethylene; (★ and ☆) butadiene; the filled and open symbols denote short and long pulses, respectively.

(P(22)), the high-frequency side of the band, for the maximum fluence (unfocused) for these lines. The equivalent yield for the high-frequency line was unexpected and may be a consequence of the red shift of the 1067- cm^{-1} peak of the band; this has been observed for SF_5NF_2 .²⁵ The majority of the quantitative experiments were performed at 1045.0 cm^{-1} because of the ease of obtaining higher fluence.

The variation of the product branching fraction with absorbed energy (or ϕ) and pulse duration is shown in Figure 3. The ethylene yields plotted in Figure 3 are only from reaction 1a and have been corrected for ethylene generated by secondary reaction of ethyl acrylate, as discussed below. There is no obvious dependence of the product ratio on pulse length for the same absorbed energy (or fluence). The branching fraction strongly depends on absorbed energy and changes from entirely reaction 1a to a dominance by reaction 1b at $\langle E \rangle = 120$ kcal mol^{-1} .

Figure 4 depicts the individual reaction probabilities (the total reaction probability was given in Figure 2) for ethylene, 1,3-butadiene, and ethyl acrylate vs. ϕ at 0.05 torr. The reaction probability for ethyl acrylate shows a sudden break at ~ 2.8 J cm^{-2} . This peculiarity in the kinetics of the 1b channel is displayed more clearly in Figure 5, where the ratio of butadiene to ethyl acrylate is plotted vs. ϕ . The measurements for Figures 4 and 5 were performed with a single laser pulse. For $\phi \geq 2.5$ J cm^{-2} , $P(\phi)$ of 1,3-butadiene is greater than that of ethyl acrylate even though both should result from the same reaction channel. A ratio > 1 implies that there is secondary formation of 1,3-butadiene or loss of acrylate. It was strongly suspected that ethyl acrylate itself was undergoing laser-induced unimolecular reaction giving ethylene and acrylic acid as products. As one means of testing this expectation, room-temperature laser excitation (1045.02 cm^{-1}) of ethyl acrylate was briefly studied. The reaction goes very readily and $P(\phi)$ is ~ 1 at 3 J cm^{-2} ; see Figure 6. The question

(25) Lyman, J. L.; Danen, W. C.; Nilsson, A. C.; Nowak, A. V. *J. Chem. Phys.* 1979, 71, 1206.

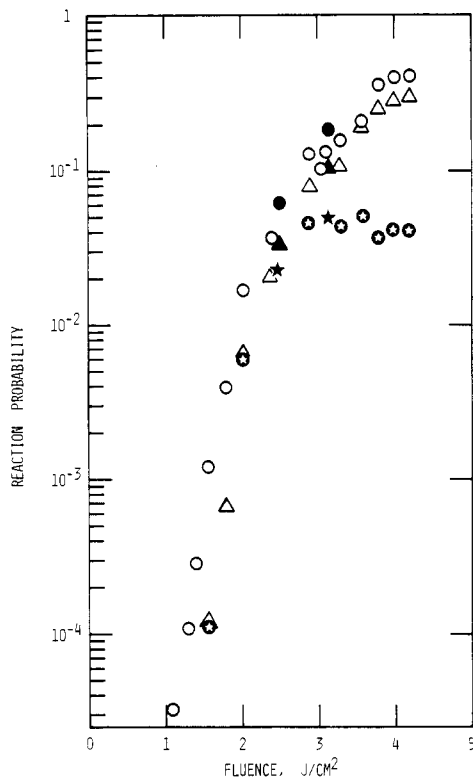


Figure 4. Individual product reaction probability for 0.05-torr experiments vs. fluence: (● and ○) ethylene; (▲ and △) butadiene; (★ and ☆) acrylate; the filled and open symbols denote short and long pulses, respectively.

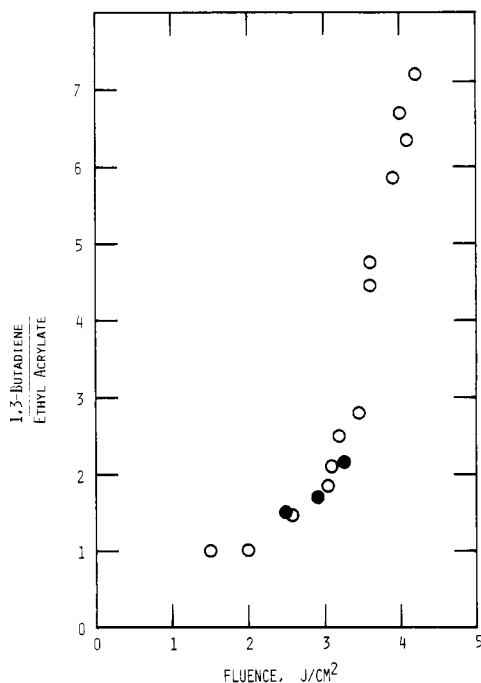


Figure 5. Ratio of 1,3-butadiene to ethyl acrylate vs. fluence for 0.05-torr experiments: (○) long pulse; (●) short pulse.

of secondary reactions is examined more closely in the Discussion section, but we do attribute the variation of the butadiene/acrylate ratio with ϕ to the secondary laser-induced decomposition of ethyl acrylate; this occurs during the same pulse that the acrylate was formed.

Bath Gas Effect. The effect of added isopropyl bromide on the [ethylene]/[butadiene] and [butadiene]/[ethyl acrylate] ratios is negligible according to the data of Table II. However, even small amounts of isopropyl bromide dramatically reduce $P(\phi)$. Figure 7 displays the quenching

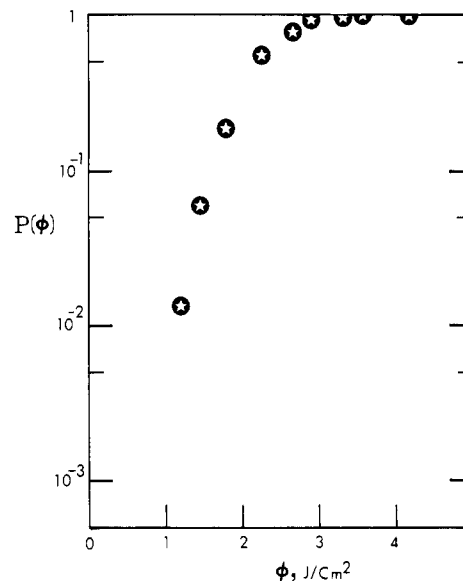


Figure 6. Reaction probability of ethyl acrylate (0.05 torr) vs. fluence for 1045.02-cm⁻¹ irradiation.

TABLE II: Effect of Added Isopropyl Bromide on Ethylene/1,3-Butadiene and 1,3-Butadiene/Ethyl Acrylate

ϕ , J cm ⁻²	isopropyl bromide, torr	Y_0/Y^a	ethylene/ 1,3- butadiene ^b	1,3- butadiene/ ethyl acrylate ^b	$P(\phi)$ - [isopropyl bromide]
2.9	0.00	1	1.6	1.7	0.00
2.8	0.10	1.9	1.6	1.7	0.0033
2.8	0.20	2.6	1.6	2.2	0.0016
2.9	0.30	3.4	1.5	2.2	0.0011
2.8	0.40	3.9	1.7	2.2	0.0009

^a Y_0 and Y are the reaction yields (total amounts of ethylene and 1,3-butadiene) without and with added isopropyl bromide, respectively, for irradiation of 0.05 torr of carboxylate. ^b Estimated uncertainty ± 0.02 .

effect graphically by means of a Stern-Volmer plot in which Y_0 is the reaction yield without added gas and Y is the reaction at a given pressure of bath gas. The addition of only ~ 0.1 torr of isopropyl bromide to 0.05 torr of carboxylate reduced $P(\phi)$ by a factor of ~ 2 at $\phi = 2.9$ J cm⁻², as shown in Figure 7A. The quenching effects of added CF₄ and He are depicted in Figure 7, B and C, respectively. Figure 8 illustrates the rather minor effect of added CF₄ and He on the ratio of ethylene to 1,3-butadiene (reaction channel 1a:1b) for several fluences. Neither gas significantly changed the product ratio, even though the absolute reaction yield may be reduced dramatically.

Energy Absorption Measurements. Beer's law behavior was observed in plots of $\log \phi/\phi_0$ vs. pressure for 0.02–0.25 torr. The energy absorption cross section, σ_L , was related to the transmittance measurements by eq 2, in which ϕ_0

$$\ln(\phi_t/\phi_0) = \sigma_L \phi N \quad (2)$$

and ϕ_t are the incident and transmitted fluences σ_L the bulk effective cross section (cm² molecule⁻¹), l the cell length, and N the concentration of the carboxylate. The measured cross section at 1045.0 cm⁻¹ is constant for $\phi \leq 4$ J cm⁻², as shown in Figure 9. In general, $\sigma_L(\phi)$ depends on fluence^{22,23} and the constancy of $\sigma_L(\phi)$, especially for $P(\phi) \geq 0.2$ ($\phi \sim 3$ J cm⁻²), is suspect since, for sufficiently high ϕ , $\sigma_L(\phi)$ must decline because of the large extent of chemical reaction during the laser pulse, which depletes the number of absorbing molecules. The absence of decline in $\sigma(\phi)$ is attributed to absorption by the ethyl acrylate

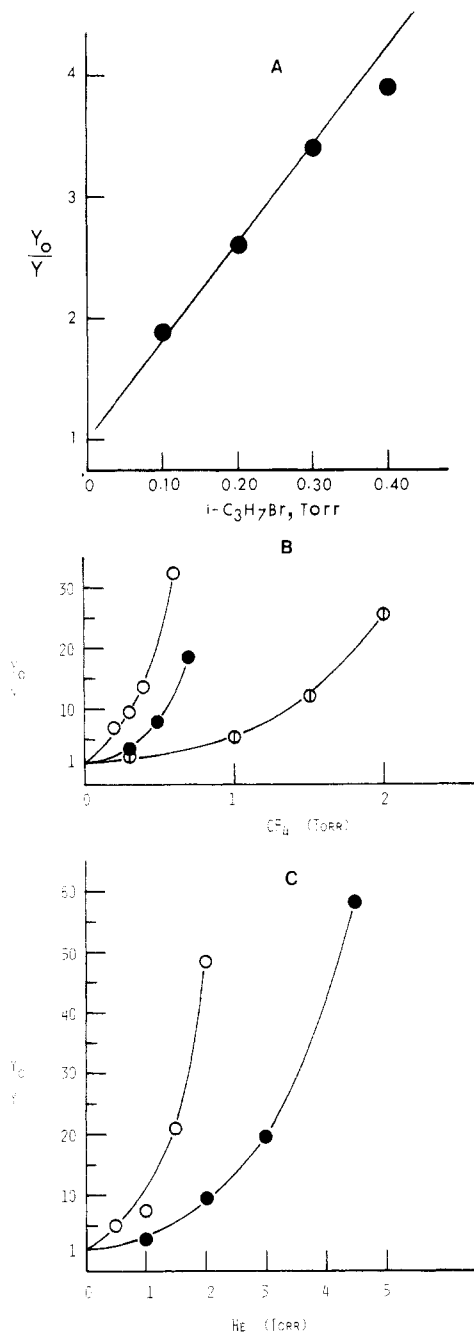


Figure 7. Reaction yield ratio from 0.10 torr of carboxylate with added $i\text{-C}_3\text{H}_7\text{Br}$, CF_4 , or He for various fluences. A: (●) 2.9 J cm^{-2} . B: (○) 1.9, (●) 2.5, (◊) 3.6 J cm^{-2} . C: (○) 2.2, (●) 3.5 J cm^{-2} . The lines (curves) connect the points and have no physical significance.

product, which has a broad-band, single-photon absorption cross section of $2.2 \times 10^{-19} \text{ cm}^2$ at 1045 cm^{-1} . From ϕ_L and ϕ_0 , the total energy absorbed per molecule, E_{abs} , can be calculated by eq 3. The E_{abs} and $\langle n \rangle$ values, which may

$$E_{\text{abs}} = \phi_0 \sigma_L \quad \langle n \rangle = \phi_0 \sigma_L / h\nu \quad (3)$$

be upper limits because of the secondary absorption, will be used for model calculations in the Discussion section.

Calculations of RRKM Rate Constants and Boltzmann Distributions. Vibrational frequencies of the carboxylate were assigned from those of cyclohexene²⁶ and ethyl acetate,²⁷⁻³⁰ and the activated complex models (Table III) were

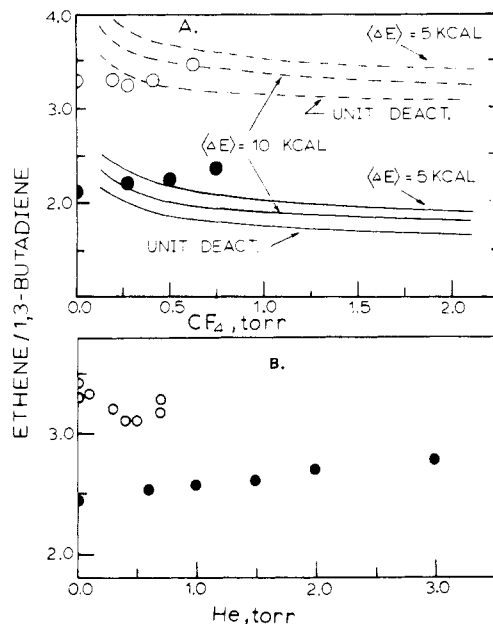


Figure 8. Ethylene/1,3-butadiene ratio from 0.10 torr of carboxylate with added CF_4 (A) and He (B) for various fluence. A: (○) 1.9, (◻) 2.5 J cm^{-2} . B: (○) 1.8, (●) 2.2 J cm^{-2} . The curves are calculated results for the strong-collision model and for stepladder model with $\langle \Delta E \rangle = 5$ and 10 kcal mol^{-1} . The curves were calculated for 1000 ($\langle E \rangle = 56 \text{ kcal mol}^{-1}$) and 1100 ($\langle E \rangle = 67 \text{ kcal mol}^{-1}$) K distributions; the $A^{\ddagger} = 7 \times 10^{14}$ model was used for channel 1b.

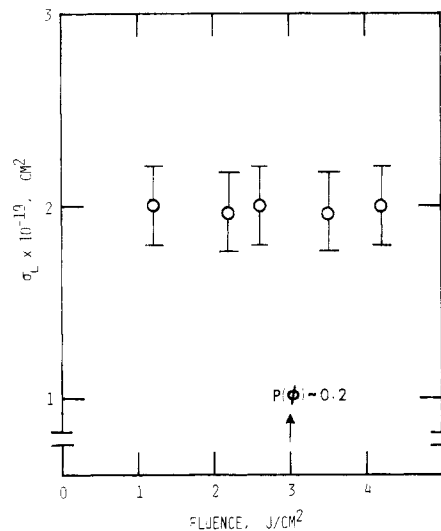


Figure 9. Laser absorption cross section, ϕ_L , vs. fluence for 1045.05 cm^{-1} . The bars indicate the experimental uncertainty associated with the reproducibility of the measurements. See text for discussion of other uncertainties in the high ϕ range.

assigned by changing the molecular frequencies to match the preexponential factors of the Arrhenius rate constants.³¹ The threshold energies, E_0 , for reactions 1a and 1b are based on the activation energies of ethyl acetate³¹ and 4-vinylcyclohexene.³¹ Using harmonic oscillator sums and densities of states, we calculated RRKM rate constants and Boltzmann distributions. Figure 10 depicts the RRKM rate constants for reactions 1a and 1b and Boltzmann distributions at five different temperatures. The

(29) Katritzky, A. R.; Lagowski, J. M.; Beard, J. A. T. *Spectrochim. Acta* 1960, 16, 954, 964.

(30) Saunders, J. E.; Lucier, J. J.; Bentley, F. F. *Appl. Spectrosc.* 1968, 22, 697.

(31) Benson, W. W.; O'Neal, H. E. "Kinetic Data on Gas Phase Unimolecular Reactions"; National Bureau of Standards: Washington, DC, 1970.

(26) Neto, N.; Di Lauro, C.; Castellucci, E.; Califano, S. *Spectrochim. Acta, Part A* 1967, 23, 1763.

(27) Shimanouchi, T. "Tables of Molecular Vibrational Frequencies"; National Bureau of Standards: Washington, DC, 1972; Vol. I.

(28) Nolin, B.; Jones, R. N. *Can. J. Chem.* 1956, 34, 1392.

TABLE III: Models for Ethyl 3-Cyclohexenecarboxylate and Transition States

	activated complexes		
	molecule	channel 1a	channel 1b ^c
frequency, cm ⁻¹	2935 (14)	2880 (14)	2935 (14)
	1405 (18)	1405 (17)	1405 (18)
	1085 (13)	1080 (12)	1100 (13)
	770 (10)	765 (12)	755 (9)
	435 (7)	430 (6)	430 (4)
	200 (4)	305 (4)	185 (4)
	90 (3)	140 (3)	95 (6)
A ^Q , s ⁻¹		3.88 × 10 ¹² ^a	7.0 × 10 ¹⁴ ^b
reaction path degeneracy		3	1
E ₀ , kcal mol ⁻¹		47	60

^a The preexponential factor in partition function form at 800 K; the Arrhenius parameters are $5.69 \times 10^{12} \text{ s}^{-1}$ and $47.6 \text{ kcal mol}^{-1}$. ^b These are the preexponential factors in partition function form at 800 K; the Arrhenius parameters are $2.7 \times 10^{15} \text{ s}^{-1}$ and 62 kcal mol^{-1} . The ratio of rotational partition functions was set as 1.2. ^c Some calculations (see Figure 11) also were done with a model with $A^Q = 4.8 \times 10^{14} \text{ s}^{-1}$; this was obtained by increasing the 95 and 185 sets of frequencies to 100 and 190 cm⁻¹, respectively.

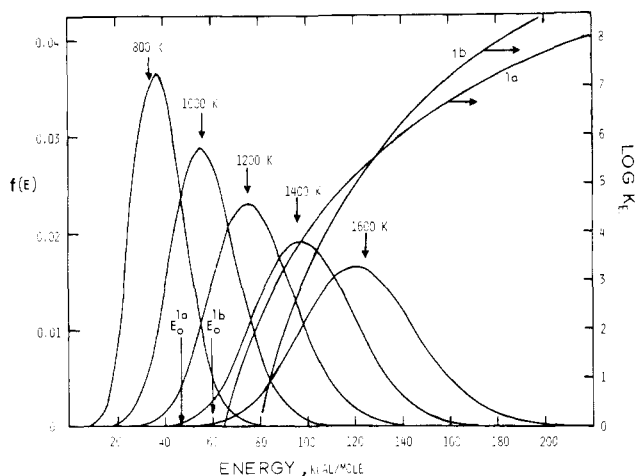


Figure 10. RRKM specific rate constants (right-hand scale) and Boltzmann distributions for ethyl 3-cyclohexene-1-carboxylate vs. energy. The rate constants shown for channel 1b are for the model with the larger preexponential factor.

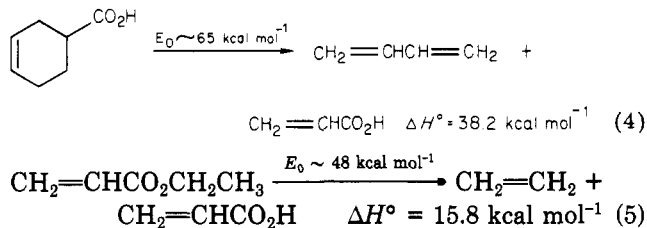
higher A factor and E_0 channel becomes increasingly competitive with the lower A factor and E_0 channel as the vibrational energy becomes larger and $k_{1a}(E) \approx k_{1b}(E)$ at 130 kcal mol⁻¹. Since the E_0 values are somewhat uncertain, the calculated rate constants have uncertainties of factors of 2–3.

In order to relate the experimental branching ratio to the RRKM rate constant ratio, one needs the distribution of activated molecules. Direct comparison of $k_{1a}(E)$ with $k_{1b}(E)$ implies a monoenergetic experimental distribution. As a model distribution, we will use a Boltzmann distribution defined by the measured absorbed energy, which gives $\langle E \rangle$ and hence the temperature. For an absorption cross section that is constant with ϕ , the resulting energy distribution is broad and similar to a Boltzmann distribution.^{1,23} We are not claiming that the real distribution is analytically Boltzmann; rather we are using it as a useful approximation to the general shape and the $\langle E \rangle$ of the real distribution. For a Boltzmann distribution the mean rate constant, $\int_0^\infty k_E F(E) dE$, is the same as the high-pressure Arrhenius rate constant. The Arrhenius rate constants for reactions 1a and 1b become equal at $\sim 1200 \text{ K}$, which corresponds to $\langle E \rangle \sim 80 \text{ kcal mol}^{-1}$. Of course, the mean

energy of the reacting molecules is much higher and will be near the 130 kcal mol⁻¹ figure mentioned in the above paragraph.

Discussion

Secondary Reactions. Figure 5 shows that the 1,3-butadiene yield exceeds the acrylate yield at $\phi > 3 \text{ J cm}^{-2}$, even though both products should be generated in equal amounts via reaction 1b. Another observation indicating a secondary reaction is that the apparent total reaction probability exceeds unity at $\phi > 5 \text{ J cm}^{-2}$. The possible explanations are (a) subsequent decomposition (reaction 4) of 3-cyclohexene-1-carboxylic acid yielding butadiene



or (b) the decomposition of ethyl acrylate yielding ethene. Evidence for the secondary reaction of acrylates (reaction 5) is the decline in $P(\phi)_{\text{acrylate}}$ for $\phi \gtrsim 3 \text{ J cm}^{-2}$ and the concomitant increase in $P(\phi)_{\text{ethene}}$. The next question is whether reaction 5 is laser driven, i.e., the acrylate reacts following absorption of photons, or whether acrylate is formed via reaction 1b with enough vibrational energy to directly undergo reaction. Since these are single-pulse experiments, reaction of cold ethyl acrylate by subsequent laser pulses need not be considered. Also, postpulse thermal reaction of ethyl acrylate was excluded by the thermal monitor studies (Table I). Further evidence against postpulse thermal decomposition of ethyl acrylate from the carboxylate is provided in Table II by the experiment in which 0.4 torr of added isopropyl bromide produced a 3.9-fold decrease in the total reaction yield but did not appreciably affect the 1,3-butadiene/acrylate or ethylene/1,3-butadiene ratios.

An estimate of the ethyl acrylate internal energy produced via reaction 1b can be made as follows. From the RRKM k_E values (Figure 10), an energy of $\sim 115\text{--}120 \text{ kcal mol}^{-1}$ is required to produce $k_E \gtrsim 10^5 \text{ s}^{-1}$; such a rate is essential for competition with bulk cooling, which limits the reaction time to $\leq 10 \mu\text{s}$.^{22,23} Since $\Delta H^\circ(1b) \sim 37 \text{ kcal mol}^{-1}$, about 78 kcal mol⁻¹ will be partitioned between 1,3-butadiene and ethyl acrylate. If one ignores the six translational and rotational degrees of freedom of the reactant and the equivalent for the products and assumes statistical partitioning, ethyl acrylate will have $\langle E \rangle \sim 48 \text{ kcal mol}^{-1}$. For a Boltzmann distribution of this energy only $\sim 5\%$ of these molecules will decompose in the 10- μs postpulse period, according to RRKM calculations done for ethyl acrylate. In order to explain the observed 1,3-butadiene/acrylate ratio by direct reaction for an absorbed energy of 115 kcal mol⁻¹ ($\phi \sim 3.9 \text{ J cm}^{-2}$), the acrylate must acquire a very large fraction of the available energy. Although these energy-partitioning arguments are only qualitative, ethyl acrylate molecules from reaction 1b probably do not receive sufficient vibrational energy for extensive secondary unimolecular decomposition, and the secondary reaction must be largely laser driven. The same statistical argument applied to the cyclohexenecarboxylic acid channel gives $\langle E \rangle \sim 70 \text{ kcal mol}^{-1}$. Since E_0 is $\sim 65 \text{ kcal mol}^{-1}$ for this retro Diels–Alder reaction, only a small fraction of the $\langle E \rangle = 70 \text{ kcal mol}^{-1}$ distribution will have $k_E > 10^5 \text{ s}^{-1}$, because this molecule has considerably smaller rate constants than ethyl acrylate at the same values of

$\langle E \rangle - E_0$. The calculated fractional decomposition in 10 μ s for a Boltzmann distribution of cyclohexenecarboxylic acid molecules with $\langle E \rangle = 70$ kcal mol⁻¹ was 0.11. We then conclude that significant direct secondary reaction for the 1a channel is unlikely.

From the above discussion, the ethyl acrylate produced in reaction 1b must absorb additional energy from the same laser pulse from which it was generated to undergo reaction. Figure 6 shows that room-temperature ethyl acrylate does undergo laser-induced reaction when irradiated under the same experimental conditions as used for the carboxylate, and vibrationally excited ethyl acrylate certainly will absorb laser energy. Since the molecule already has about one-half of the necessary energy, the laser-driven secondary reaction is easily accomplished. Identification of such laser-induced secondary reactions is becoming common, e.g., SF₆,^{32,33} SF₅Cl,³³ CH₃CHF₂,³⁴ halogenated methanes,^{35,36} cyclobutyl chloride,³⁷ and CF₃OOCF₃.³⁸

If reaction of ethyl acrylate is the only secondary reaction, then the initial yield from channel 1a can be obtained from eq 6. $Y(\text{ethylene})_{\text{total}}$ is the yield of ethylene determined by GLPC analysis. The value in brackets is the yield of ethylene resulting from the decomposition of acrylate. Equation 6 was utilized for the calculation of the ethylene yield from channel 1a from the raw experimental data.

$Y(\text{ethylene}) = Y(\text{ethylene})_{\text{total}} - [Y(\text{butadiene}) - Y(\text{ethyl acrylate})]$ (6)

Product Ratio and Reaction Probability of Neat Reactant. Figure 3 demonstrates that the corrected ethylene to 1,3-butadiene ratio declines smoothly from >90 at a fluence of 1.0 J cm⁻², $\langle E \rangle = 34$ kcal mol⁻¹, to 0.5 at 4.2 J cm⁻², $\langle E \rangle = 126$ kcal mol⁻¹. The higher E_0 channel increasingly competes with the low E_0 channel and becomes dominant at $\langle E \rangle \geq 100$ kcal mol⁻¹. The general results are consistent with the RRKM rate constants, which predict a crossover in reaction channels as the energy in the parent molecule is increased to ~ 140 kcal mol⁻¹. This gain in the high E_0 channel is a consequence of its much looser transition state (larger preexponential factor). This general match between the calculated and experimental branching ratios is taken as evidence that the absorbed energy is randomized in the carboxylate. The next step is to incorporate a distribution into a model calculation in an attempt to obtain a better understanding of the dependence of k_{1a}/k_{1b} on absorbed energy.

The data in Figure 3 also show that the laser pulse duration had a negligible effect on the branching ratio in contrast to the results with ethyl vinyl ether.¹² The variation in the ethylene/1,3-butadiene ratio with fluence definitely establishes that the mean excitation level of the reacting molecules increases with fluence. This differs from the interpretation of the results on the two-laser irradiation of OsO₄ in which an increase in fluence only caused excitation of a greater fraction of molecules but did not seriously affect the ultimate level of excitation.³⁹ In

our interpretation of the absorbed energy and in the model calculations to follow, we have assumed that all molecules have the same probability for absorption of photons from the radiation field; i.e., there are no vibrational or rotational bottlenecks.

Calculation of Product Yield Ratio. For $P(\phi) \lesssim 0.1$ the k_E values are $< 10^6$ s⁻¹ for a large fraction of the molecules in the distribution and most of the reaction occurs after termination of the laser pulse.^{1,23} For samples with no inert bath gas, the quenching of the postpulse reaction is determined by the time period required for cooling of the irradiated volume.^{22,23} This feature results from the combination of two properties of large molecules: (i) the fact that all, or nearly all, molecules in the irradiated volume absorb laser energy and (ii) the small heat capacity of the translational and rotational degrees of freedom, relative to the vibrational heat capacity. Although complicated by several factors, the virtual independence of $P(\phi)$ on parent gas pressure is one demonstration of the importance of the bulk cooling of the irradiated volume rather than collision with parent gas for quenching the laser-initiated reaction. If an inert bath gas is added, then bath gas collisions do constitute the limiting time for postpulse reaction and this is why quenching is observed for such experiments. For higher fluence with $P(\phi) > 0.1$, molecules reach sufficiently high energy that $k_E \geq 10^6$ s⁻¹ and reaction during the pulse must be included in the modeling.²³

For experiments dominated by postpulse reaction, the ratio of reaction via channels 1a and 1b can be calculated by averaging the respective reaction probabilities over the appropriate distribution function. Master equation modeling^{1,22,23} for molecules with $\sigma_L(\phi)$ similar to that of the carboxylate show that a Boltzmann distribution with $\langle E \rangle = nh\nu + \langle E \rangle_{\text{thermal}}$, the absorbed laser energy plus the initial thermal energy, closely resembles the actual calculated distribution. Therefore, $F(E)$ in eq 7 and 8 were taken as

$$r = \int_{E_0^{1a}}^{\infty} \frac{k_E^{1a}}{k_E^{1a} + k_E^{1b} + 1/\tau} F(E) dE / \int_{E_0^{1b}}^{\infty} \frac{k_E^{1b}}{k_E^{1a} + k_E^{1b} + 1/\tau} F(E) dE \quad (7)$$

a Boltzmann distribution. τ is the mean time before bulk cooling quenches the reaction. If $\tau^{-1} > k_E^{1a} + k_E^{1b}$, eq 7 reduces to eq 8, and r becomes the ratio of the high-

$$r = \int_{E_0^{1a}}^{\infty} k_E^{1a} F(E) dE / \int_{E_0^{1b}}^{\infty} k_E^{1b} F(E) dE = A_{1a}^Q / A_{1b}^Q \exp[-(E_0^{1a} - E_0^{1b})RT] \quad (8)$$

pressure limiting rate constants for the two channels. The superscript Q denotes preexponential factors in partition function form. For the higher-energy distributions, the full average must be calculated, since $k_E \approx \tau^{-1}$. We actually used both Boltzmann and Poisson distributions to calculate r ; however, the calculated average RRKM rate constant ratios, $\langle k_E^{1a} \rangle / \langle k_E^{1b} \rangle$, vs. average excitation energy, $\langle E \rangle$, did not differ significantly for the Boltzmann (broad) or Poisson (narrow) energy distributions. Consequently, we utilized a Boltzmann distribution for comparison with the data.

The calculated results from both eq 7 and 8 are compared with the experimental results in Figure 11. The $P(\langle E \rangle)$ values are indicated at the top of Figure 11 and only data with $P(\langle E \rangle) \lesssim 0.3$ are shown since, for larger

(32) Grant, E. R.; Coggiola, M. J.; Lee, Y. T.; Schulz, P. A.; Sudbo, Aa. S.; Shen, Y. R. *Chem. Phys. Lett.* 1977, 52, 595.

(33) Presses, J. M.; Weston, R. E., Jr.; Flynn, W. G. *Chem. Phys. Lett.* 1977, 48, 425.

(34) Quick, C. R., Jr.; Wittig, C. J. *Chem. Phys.* 1978, 69, 4201.

(35) Wurzburg, E.; Kovalenko, L. J.; Houston, P. L. *Chem. Phys.* 1978, 35, 317.

(36) Sudbo, Aa. S.; Schulz, P. A.; Grant, E. R.; Shen, Y. R.; Lee, Y. T. *J. Chem. Phys.* 1979, 70, 912.

(37) Francisco, J. S.; Steinfeld, J. I. *Int. J. Chem. Kinet.* 1981, 13, 615.

(38) Francisco, J. S.; Findeis, M. A.; Stienfeld, J. I. *Int. J. Chem. Kinet.* 1981, 13, 627.

(39) Ambartzumian, R. V.; Makarov, G. N.; Poretzky, A. A. *Opt. Commun.* 1978, 27, 79.

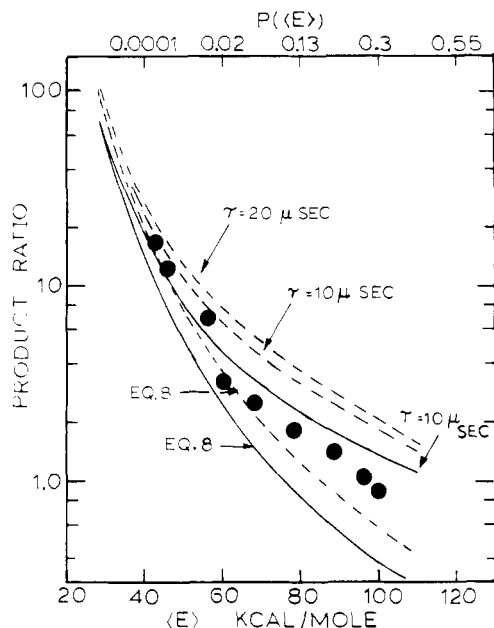


Figure 11. Comparison of experimental (●) and calculated product yield ratios vs. absorbed energy. The two sets of curves are for the two choices of transition-state models for channel 1b: $A^{\ddagger} = 7.0 \times 10^{14} \text{ s}^{-1}$, (—); $A^{\ddagger} = 4.8 \times 10^{14} \text{ s}^{-1}$ (---). The two lowest curves are calculated from eq 8. The other curves are from eq 7 with the indicated cooling times, τ .

extents of reaction, processes occurring during the pulse must be included. For cooling times of $<10 \mu\text{s}$, the difference between eq 7 and 8 reaches a factor of 3 at $\langle E \rangle \sim 100 \text{ cal mol}^{-1}$. Larger τ enhances the reaction probability of low-energy molecules and thus r increases with increasing τ at a given $\langle E \rangle$. For $\langle E \rangle$ above $\sim 60 \text{ kcal mol}^{-1}$ it is desirable to use eq 7. Within the experimental uncertainty of $E_0^{1a} - E_0^{1b}$, the model calculations are certainly in agreement with the data for realistic values of τ ($\leq 10 \mu\text{s}$). The uncertainty in $E_0^{1a} - E_0^{1b}$ is at least 2 kcal mol^{-1} , which corresponds to a shift of the curves by a factor of 3.4 and 2.3 at $\langle E \rangle = 40$ and 80 kcal mol^{-1} , respectively. Inspection of Figure 10 shows that, in the range where $k_E^{1a} + k_E^{1b} \approx 10^6 \text{ s}^{-1}$, $k_E^{1b} > k_E^{1a}$ and the component of reaction occurring during the pulse contributes a ratio of channels < 1.0 . This corresponds to the trend observed in Figure 2 and the ratio reaches ~ 0.5 at $\langle E \rangle = 120 \text{ kcal mol}^{-1}$. The model employed depends only on the absorbed energy and, hence, predicts no dependence of r on intensity, which is in agreement with the experimental results.

There now are several^{12,22,40-46} documented studies that demonstrate the expected RRKM product branching from MPA. Most measurements are for a rather restricted range of ϕ (or $\langle E \rangle$). Our work is one of the first to show a large change in the product ratio, from 90 to 0.5, for a measured range of $\langle E \rangle$. In addition to verifying statistical distribution of intramolecular energy, the data are fully in ac-

cord with the master equation treatment of photon absorption leading to a broad energy distribution.^{22,23} In this context the work with ethyl vinyl ether¹² is puzzling. The product ratio follows the RRKM expectation; however, the product ratio is dependent on laser intensity as well as fluence. This suggests the presence of a bottleneck in the vibrational manifold of levels. We have found no evidence for a vibrational bottleneck for the cyclohexene-1-carboxylate; however, there may be rotational restrictions to laser photon absorption at low ϕ ; see next section.

Calculations of $P(\phi)$ in Absence of Bath Gas. The calculated (eq 7) absolute reaction probability values are compared with the experimental results in Figure 2 for $P(\langle E \rangle) \leq 0.3$. The calculated absolute yields depend much more critically on the values selected for τ and upon the absolute values of k_E and poorer agreement with experimental results is expected than for the product ratio r . Modest agreement is found for a cooling time of $20 \mu\text{s}$ for $P(\phi) = 0.01-0.1$. For $P(\phi) < 0.01$ longer cooling times are required. Such times are unrealistic and, in fact, are experimentally ruled out from the absence of thermal reaction of the added thermal monitor. Below $P(\langle E \rangle) = 0.01$ the reaction is surely postpulse. Several factors could be important that are not in our model; we have suggested elsewhere²³ that fluence-dependent rotational fractionation during the absorption process may be important even for large molecules. Rotational fractionation will result in higher $P(\phi)$ at a given ϕ because, if only a fraction, f , of the molecules are absorbing the laser energy, the mean energy of the subensemble absorbing the energy is $\langle E \rangle / f$. Brenner⁴⁷ also has discussed the difficult problems associated with explaining the large fraction of molecules interacting with the CO_2 laser.

Reaction Probability and Product Ratio with Added Bath Gases. Equation 7 can be used to estimate the reaction probability in the presence of bath gases, if τ^{-1} is replaced by the collisional frequency, ω . In this form the model corresponds to the strong-collision assumption; however, more elaborate deactivation models²³ can be included if desired. A new complication that arises from experiments with bath gas, even if the yield is dominated by postpulse reaction and eq 7 is applicable, is the effect of collisions during the pulse on the energy distribution function and $\langle E \rangle$. Experiments were done with constant CF_4 (0.1 torr of carboxylate and 0.5 torr of CF_4) pressure but variable ϕ in order to avoid the need to calculate the absolute $P(\phi)$ for the neat sample. Direct comparison can be made between the calculated and measured $P(\langle E \rangle)$ in the presence of CF_4 for a range of $\langle E \rangle$ by employing eq 7 or a suitable modification for more realistic collisional deactivation. The absorbed energy was calculated by assuming that $\sigma_L(\phi)$ with 0.6 torr of CF_4 are the same as for neat carboxylate. The assumption is reasonable since $\sigma_L(\phi)$ for ethyl fluoroacetate was unaffected²³ by 1.5 torr of CF_4 and the addition of He and N_2 up to 10 torr did not affect $\sigma_L(\phi)$ of cyclobutyl acetate.⁴⁵ The collisional frequency between CF_4 and carboxylate ($1.2 \times 10^7 \text{ s}^{-1} \text{ torr}^{-1}$) indicates that approximately seven collisions will occur during the $\sim 1\text{-}\mu\text{s}$ laser pulse, even though $\sigma_L(\phi)$ may be unaffected by 0.6 torr of CF_4 , some collisional energy transfer to CF_4 will occur during the laser pulse and the calculated $\langle E \rangle$ will be an upper limit to the true value. Since the pressure of CF_4 was constant for these experiments, the calculated $\langle E \rangle$ values for the series of experiments should be realistic on a relative scale. A comparison between experimental and calculated $P(\langle E \rangle)$ vs. $\langle E \rangle$ is shown in Figure 12 for

(40) Lawrance, W. D.; Silverstein, J.; Zang, F. M.; Shu, Q. S.; Francisco, J. S.; Steinfeld, J. I. *J. Phys. Chem.* 1981, 85, 1961.

(41) Wanna, J. T.; Tardy, D. C. *J. Phys. Chem.* 1981, 85, 3749.

(42) Richardson, T. H.; Setser, D. W. *J. Phys. Chem.* 1977, 81, 2301.

(43) (a) Harrison, R. G.; Hawkins, H. L.; Leo, R. M.; John, P. *Chem. Phys. Lett.* 1980, 70, 555. (b) Storov, V.; Selamoglu, H.; Steel, C. *J. Phys. Chem.* 1981, 85, 320. (c) Back, M. H.; Back, R. A. *Can. J. Chem.* 1979, 57, 1511. Other workers, (ref 43, a and b) have not been able to reproduce some of the data reported here.

(44) Farneth, W. E.; Thomsen, M. W.; Schultz, H. L.; Davies, M. A. *J. Am. Chem. Soc.* 1981, 103, 4001.

(45) Nguyen, H. H.; Danen, W. C.; Setser, D. W., Manuscript in preparation.

(46) Papagiannakopoulos, P. J.; Kostnik, K.; Benson, S. W. *Int. J. Chem. Kinet.* 1982, 14, 327.

(47) (a) Brenner, D. M. *J. Chem. Phys.* 1981, 74, 2293. (b) Brenner, D. M.; Brezinsky, K.; Curtis, P. M. *Chem. Phys. Lett.* 1980, 72, 202.

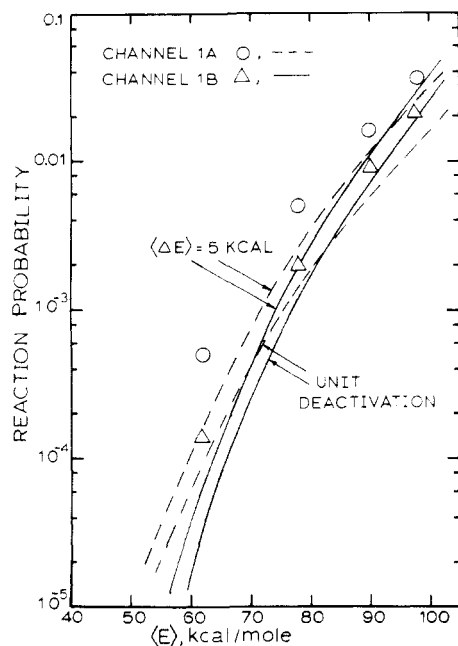


Figure 12. Comparison between calculated and experimental reaction probability vs. $\langle E \rangle$ for experiments with CF_4 buffer gas (0.10 torr of carboxylate + 0.60 torr of CF_4). The curves show the calculated results for strong-collision and stepladder deactivation models, $\langle \Delta E_d \rangle = 5 \text{ kcal mol}^{-1}$. The calculated and experimental results are shown for each channel. The $A^{\ddagger} = 7.0 \times 10^{14} \text{ s}^{-1}$ transition-state model was used for channel 1b.

unit collisional deactivation calculated with $\omega = 1.2 \times 10^7 \text{ s}^{-1} \text{ torr}^{-1}$ and stepladder collisional deactivation with $\langle \Delta E \rangle = 5 \text{ kcal mol}^{-1}$; the latter is in the expected range of the mean energy lost per collision based on chemical activation data.⁴⁸⁻⁵⁰ The stepladder calculation gives increased yields for both channels relative to unit deactivation results as expected. The increase is somewhat greater for the lower threshold energy channel; thus, the increase for channel 1a is approximately a factor of 2 while that for channel 1b is less than a factor of 2. One consequence of this difference is that higher energy is required before the yields of the two channels become equal for the stepladder model relative to the unit deactivation model. The $\langle \Delta E \rangle = 5 \text{ kcal mol}^{-1}$ stepladder calculation is in modest agreement with the data, especially for channel 1b. The general agreement between the calculated and experimental results is strong evidence that the limiting process to the reaction yield is CF_4 collisions rather than bulk cooling. Considering the simplicity in the model, the good agreement with the absolute yield and the energy dependence of the yields are pleasing.

The addition of He had little effect on the product ratio for several fluences and pressures, although considerable quenching was observed; see Figure 8. The addition of 0.6 torr of CF_4 at $\phi = 1.9 \text{ J cm}^{-2}$ reduced the yield by a factor of 32 but the ratio of channel 1a to 1b was affected only slightly (Figure 8); no significant secondary reaction occurs at this fluence (Figure 5). At 2.5 J cm^{-2} the ethylene/butadiene ratio appeared to increase slightly with added CF_4 , indicating a possible preferential quenching to the higher E_a channel; however, the trend is within the experimental uncertainty and the main conclusion is that the ratio is virtually independent of CF_4 pressure. We have

observed a similar independence of product channel ratio with added bath gas for cyclobutyl acetate, another large, dual-channel organic molecule.⁴⁵ These experiments display the expected behavior for a multiple-channel molecule with statistical reaction probabilities for which there are no vibrational or rotational bottlenecks in the photon absorption processes. Similar weak dependence of the product branching ratio on bath gas pressure has been observed for vinylcyclopropane,⁴⁴ cyclobutanone,⁴³ and $\text{CH}_2\text{DCH}_2\text{Cl}$ ⁴⁶ even though varying degrees of bottlenecking in the absorption are suspected for these molecules.

Some stepladder deactivation calculations were done vs. collision frequency with the postpulse model to illustrate the weak dependence of the branching ratios for the carboxylate on bath gas pressure. The calculated ethylene/1,3-butadiene ratios for $\langle E \rangle = 56$ (1000 K) and 67 (1100 K) kcal mol^{-1} for unit and stepladder deactivation with $\langle \Delta E_d \rangle = 10$ and 5 kcal mol^{-1} are shown in Figure 8A. These $\langle E \rangle$ approximately correspond to the experimental absorbed energies (55 and 71 kcal mol^{-1}) for $\phi = 1.9$ and 2.5 J cm^{-2} , respectively. The collision frequency was taken as that for CF_4 , $1.2 \times 10^7 \text{ s}^{-1} \text{ torr}^{-1}$. For the stepladder deactivation the low E_0 channel is enhanced somewhat more than the high E_0 channel relative to unit deactivation; hence, the product ratio increases slightly as $\langle \Delta E \rangle$ becomes smaller. Nevertheless, the ratio declines with increasing pressure for all model calculations because the mean energy of reacting molecules increases as the pressure increases and the k_{1a}/k_{1b} ratio monotonically declines with increasing energy. At high pressures the unit deactivation result ultimately reaches the ratio given by eq 8; see Figure 11. Below 0.3 torr of CF_4 , both bulk cooling and collisional quenching probably are important and only the calculated results above 0.3 torr should be compared to the data. For $\langle E \rangle = 67 \text{ kcal mol}^{-1}$ stepladder deactivation with $\langle \Delta E_d \rangle \approx 5 \text{ kcal mol}^{-1}$ is in moderate agreement with the results at 0.5 torr; however, the experimental ratios do not decline with increasing pressure. The calculated results for $\langle E \rangle = 56 \text{ kcal mol}^{-1}$ are slightly too high for $\langle \Delta E \rangle = 5 \text{ kcal mol}^{-1}$. The reasons could be improper $\langle E \rangle$ selection or a slightly incorrect choice of $E_0(1a)$ vs. $E_0(1b)$. The significant feature of the calculations with CF_4 is that the calculated ratio is rather insensitive to the collisional deactivation model in agreement with the experimental results. Similar conclusions have been obtained from chemical activation studies⁵⁰ of multiple reaction channel unimolecular reactions and rather extreme pressure ranges are required to see a strong variation of the product ratio on pressure even for inefficient collisional deactivation. One should note that the present experiments correspond to low reaction yield, or, in chemical activation terminology, these measurements are in the high-pressure regime. The consequences of cascade collisional deactivation are much more apparent in the low-pressure regime⁴⁸⁻⁵⁰ and this also partly explains the rather low sensitivity of the present calculations to the collision model.

The negligible effect of bath gas on the product ratio can be explained qualitatively by examining the results at $\phi = 2.5 \text{ J cm}^{-2}$. At this fluence, the energy absorbed by carboxylate is $\sim 71 \text{ kcal mol}^{-1}$ and the ethylene/butadiene product ratio is ~ 2 and $P(\langle E \rangle)$ is ≈ 0.1 . An energy of 71 kcal mol^{-1} corresponds to the $\sim 1100 \text{ K}$ distribution of Figure 10. There is a negligible fraction of molecules with $E \geq 140 \text{ kcal mol}^{-1}$, and very few molecules have sufficient energy to react during the laser pulse. After termination of the pulse, reaction occurs in competition with CF_4 collisions. One collision will, on the average, remove 5-10

(48) Marcoux, P. J.; Setser, D. W. *J. Phys. Chem.* 1978, 82, 97.

(49) Tardy, D. C.; Rabinovitch, B. S. *Chem. Rev.* 1977, 77, 369.

(50) (a) Tardy, D. C.; Larson, C. W.; Rabinovitch, B. S. *Can. J. Chem.* 1968, 46, 341. (b) Larson, C. W.; Rabinovitch, B. S. *J. Chem. Phys.* 1969, 51, 2293.

kcal mol⁻¹ of energy and greatly reduce the subsequent reaction probability. The net effect is that only molecules in the energy range of 110–140 kcal mol⁻¹ contribute to the yield, and the k_E^{1a}/k_E^{1b} ratio is 2–0.7 in this range. Although molecules undergoing collisional cascade have enhanced k_E^{1a}/k_E^{1b} ratios, their absolute reaction probability is very low and they do not contribute much to the total yield.

The most significant aspect of the bath gas experiments is the satisfactory agreement with the calculations using simple collisional deactivation models for both the reaction probabilities vs. absorbed energy and the lack of a dependence of the product yield ratio on bath gas pressure. Conversely, the comparison of results with and without bath gas imply the necessity for including a characteristic quenching time to limit the extent of reaction. This quenching time is associated with the collective processes which cool the irradiated volume.

Summary

The infrared multiphoton laser-induced reaction of ethyl 3-cyclohexene-1-carboxylate, a large molecule with dual reaction channels, provides insight into the laser-driven unimolecular reactions of large molecules which have no apparent bottleneck to multiphoton absorption of CO₂ laser energy.

(1) The reaction probability was independent of parent pressure in the range of 0.020–0.20 torr; studies with a thermal monitor molecule showed the absence of a thermal contribution to reaction below 0.1 torr.

(2) The absorption cross section, which was measured from $\phi = 1.0$ to 4.0 J cm⁻², was invariant to fluence; this may be due in part to absorption by a product formed during the same laser pulse.

(3) The absolute reaction yields and the product channel ratio were very dependent on incident laser fluence (absorbed energy); the ratio varied from >90 at 1.0 J cm⁻² to 0.5 at 4.2 J cm⁻².

(4) The reaction yield and product ratio were independent of the laser pulse duration (intensity) at constant fluence.

(5) At relatively high fluence, significant secondary reaction of the ethyl acrylate product was observed in single-pulse experiments. Vibrationally excited ethyl acrylate formed in the primary reaction channel 1b absorbs additional photons from the same laser pulse, inducing further unimolecular reaction.

(6) The addition of a bath gas reduced the absolute yield indicating that collisional quenching of excited molecules was competitive with reaction.

(7) The product ratio was virtually independent of added He, CF₄, or *i*-C₃H₇Br bath gas.

(8) The experimental yield and product ratio and the effect of bath gas on the yield and product ratio were compared to calculations using a postpulse model employing RRKM rate constants and a broad energy distribution (defined for convenience to be a Boltzmann distribution with $\langle E \rangle$ equal to the absorber laser energy). Satisfactory agreement is obtained for the regime with $P(\langle E \rangle) \leq 0.1$.

Acknowledgment. This work was supported by the U.S. National Science Foundation under grants 77-21380 and 77-22645. We thank T. S. Lee for assistance with some of the calculations.

Registry No. CH₃CHBrCH₃, 75-26-3; C₂H₄, 74-85-1; C₄H₆, 106-99-0; C₃H₆, 115-07-1; ethyl 3-cyclohexenecarboxylate, 55510-68-4; ethyl acrylate, 140-88-5.

Vibrational Relaxation within Mixed Electronic States

Alan E. W. Knight

School of Science, Griffith University, Nathan, Brisbane, Qld 4111 Australia

and Charles S. Parmenter*

Department of Chemistry, Indiana University, Bloomington, Indiana 47405 (Received: August 18, 1982;

In Final Form: October 12, 1982)

The efficiency of collisional vibrational relaxation within a fluorescing state of a polyatomic molecule is discussed for cases where the fluorescing state is of mixed electronic character involving both a radiative and nonradiative state. It is shown that the efficiency of vibrational relaxation should be changed from that within the pure radiative state by the factor A_1^2 , where A_1 is the fraction of radiative state character in the mixed electronic state. Severe reductions in vibrational relaxation efficiencies are predicted, and they are likely to occur in polyatomics whose fluorescence decay is consistent with the strong coupling, intermediate case of radiationless transition theory. Pyrimidine and pyrazine are proposed as examples. Analysis of pyrimidine data in particular shows that S₁ vibrational relaxation efficiencies are reduced by at least two orders of magnitude from those commonly found for relaxation within pure S₁ states. Such a reduction is consistent with the theory when the (known) mixed single-triplet character of the pyrimidine fluorescing state is considered.

Introduction

The observed cross sections σ_{obsd} for level-to-level vibrational transfers within the S₁ state of benzene vapor as well as for transfers into fields of S₁ levels are large.¹⁻⁴

Transfer efficiencies $P \equiv \sigma_{\text{obsd}}/\sigma_{\text{hs}}$ near or exceeding unity occur for a variety of collision partners. Accumulating experience with S₁ aniline,⁵ S₁ *p*-difluorobenzene,⁶ and S₀

(1) C. S. Parmenter and K. Y. Tang, *Chem. Phys.*, **27**, 127 (1978).
 (2) G. H. Atkinson, K. Y. Tang, and C. S. Parmenter, *J. Chem. Phys.*, **71**, 68 (1979).

(3) L. M. Logan, I. Buduls, A. E. W. Knight, and I. G. Ross, *J. Chem. Phys.*, **72**, 5667 (1980).

(4) K. Y. Tang and C. S. Parmenter, *J. Chem. Phys.*, in press.

(5) D. A. Chernoff and S. A. Rice, *J. Chem. Phys.*, **70**, 2521 (1979).